

The Extrema Edges

Pablo Andrés Arbeláez and Laurent D. Cohen

CEREMADE, UMR CNRS 7534 Université Paris Dauphine,
Place du maréchal de Lattre de Tassigny,
75775 Paris cedex 16, France
arbelaez@ceremade.dauphine.fr, cohen@ceremade.dauphine.fr

Abstract. We present a new approach to model edges in monochrome images. The method is divided in two parts: the localization of possible edge points and their valuation. The first part is based on the theory of minimal paths, where the selection of an energy and a set of sources determines a partition of the domain. Then, the valuation is obtained by the creation of a contrast driven hierarchy of partitions. The method uses only the original image and supplies a set of closed contours that preserve semantically important characteristics of edges.

1 Introduction

The presence of sharp discontinuities in the image intensity seems to play a fundamental role for the interpretation of visual information in humans. Therefore, edge detection has been a very active field of research since the early days of computer vision. Originally, edge detection techniques were motivated by the generalization to the plane of signal processing methods and the adaptation of regular analysis tools to the discrete domain. Thus, differentiation appeared as the natural operation to address the problem. Many estimations of the image derivatives and models for the edges have been proposed in the last decades. Examples include the zero crossings of the Laplacian [22], the maxima in the gradient direction [4] and the crest lines of the gradient's modulus. However, in spite of their diversity, the strategy in many edge detection methods consists in a differential approach and the use of local image information to measure the relevance of the edge points [30, 10].

The classical approach to address this issue in the context of mathematical morphology is the characterization of edges as the watershed lines of the gradient's modulus [2, 31]. Among the reasons for the large popularity of this method one can cite its intuitive definition, efficient algorithms for its implementation and the fact that the watersheds supply a set of closed edges. In the regular framework, the watersheds were defined as the skeleton by influence zones of a determined distance function [27]. These ideas inspired a construction of the watersheds using curve evolution [21].

The proposed approach to model the edges in an image follows the opposite direction. Our starting point is the theory of minimal paths, described in Section 2, where a partition of the domain is determined by the choice of an

energy and a set of sources. In Section 3, we introduce an energy called the *path variation*, a generalization of the one dimensional total variation for functions of two variables. This energy preserves the geometric structure of the function and allows to work directly on the original image. In Section 4, the choice of the intensity extrema as sources provides a piecewise constant simplification of the image, whose discontinuities are designated as the *extrema edges* of the image. Finally, in Section 5, we consider the valuation of the extrema edges using global image information. For this purpose, a family of nested partitions, guided by a notion of contrast, is constructed.

2 Minimal Paths and Energy Partitions

This introductory section presents the mathematical framework for the rest of the paper. Basic definitions are recalled and the notations settled.

Let $\Omega \subset \mathbb{R}^2$ be a compact connected domain in the plane and $x, y \in \Omega$ two points. A *path* from x to y designates a continuous function $\gamma : [a, b] \rightarrow \Omega$ such that $\gamma(a) = x$ and $\gamma(b) = y$. The image of γ is then a curve in Ω . If $\gamma \in \mathcal{C}^1([0, L])$ and we consider an arc-length parametrization of γ (i.e. $\|\dot{\gamma}(s)\| = 1, \forall s \in [0, L]$), then L represents the Euclidean length of the path and its image is a rectifiable simple curve. The set of paths from x to y is noted by Γ_{xy} and the set of paths in Ω is noted by Γ_Ω .

Definition 1. *The **surface of minimal action, or energy**, of a potential function $P : \Omega \times \mathcal{S}^1 \rightarrow \mathbb{R}^+$ with respect to a source point $x_0 \in \Omega$, evaluated at x , is defined as*

$$E_0(x) = \inf_{\gamma \in \Gamma_{x_0x}} \int_0^L P(\gamma(s), \dot{\gamma}(s)) ds .$$

When P depends only on the position $\gamma(s)$ and is strictly positive, the computation of the energy can be performed using Sethian's *Fast Marching* method [33], as detailed in [6].

The surface of minimal action with respect to a set of sources $S = \{x_i\}_{i \in J}$ is defined as the minimal individual energy:

$$E_S(x) = \inf_{i \in J} E_i(x) .$$

In the presence of multiple sources, a valuable information is provided by the interaction in the domain of a source x_i with the other elements of S , which is expressed through its *influence zone*:

$$Z_i = \{x \in \Omega \mid E_i(x) < E_j(x), \forall j \in J\} .$$

Thus, the influence zone, or briefly the *zone*, is a connected subset of the domain, completely determined by the energy and the rest of the sources. Their union is noted by:

$$Z(E, S) = \bigcup_{i \in J} Z_i .$$

The *medial set* is defined as the complementary set of $Z(E, S)$:

$$M(E, S) = \{x \in \Omega \mid \exists i, j \in J, i \neq j : E_S(x) = E_i(x) = E_j(x)\} .$$

Therefore, the selection of an energy and a set of sources defines an *energy partition* $\Pi(E, S)$ of the domain:

$$\Pi(E, S) = Z(E, S) \cup M(E, S) .$$

Energy minimizing paths have been used to address several problems in the field of computer vision, where the potential is generally defined as a function of the image. Examples include the global minimum for active contour models [6], shape from shading [17], continuous scale morphology [18], virtual endoscopy [8] and perceptual grouping [5].

3 The Path Variation

In the usual approach for the application of minimal paths to image analysis, a large part of the problem consists in the design of a relevant potential for a specific situation and type of images. However, we adopt a different perspective and use the notions of the previous section for the study of a particular energy, whose definition depends only on geometric properties of the image.

3.1 Definition

For functions of one real variable, the variation is a functional with known properties [14, 29]. It was introduced by Jordan [16] as follows:

Let $f : [0, L] \rightarrow \mathbb{R}$ be a function, $\sigma = \{s_0, \dots, s_n\}$ a finite partition of $[0, L]$ such that $0 = s_0 < s_1 < \dots < s_n = L$ and Φ the set of such partitions.

The *variation*, or *total variation*, of f is defined as

$$v(f) = \sup_{\sigma \in \Phi} \sum_{i=1}^n |f(s_i) - f(s_{i-1})| .$$

If $f \in C^1([0, L])$, then the variation can be expressed as:

$$v(f) = \int_0^L |f'(s)| ds . \quad (1)$$

The path variation is a generalization of the total variation for two variable functions:

Definition 2. The *path variation* of a function $u : \Omega \subset \mathbb{R}^2 \rightarrow \mathbb{R}$ with respect to a source point $x_0 \in \Omega$, evaluated at x , is defined as

$$V_0(u)(x) = \inf_{\gamma \in \Gamma_{x_0 x}} v(u \circ \gamma) .$$

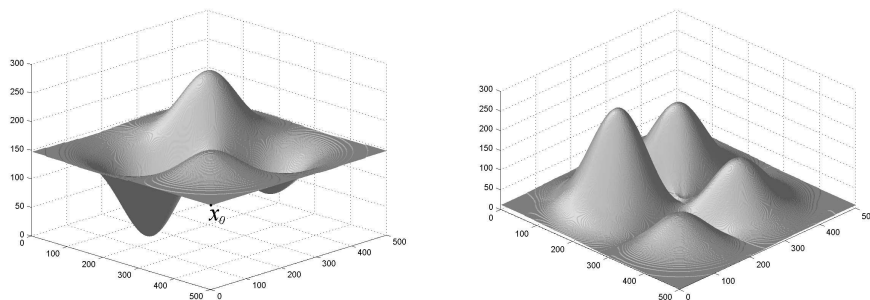


Fig. 1. Simple example: graphs of u and $V_0(u)$.

Thus, the path variation between two points is given by the minimal variation of the function on all the paths that join them.

Definition 3. The space of functions of **bounded path variation** of Ω , noted by $BPV(\Omega)$ is defined by

$$BPV(\Omega) = \{u : \Omega \rightarrow \mathbb{R} \mid \forall x_0, x \in \Omega, \exists \hat{\gamma} \in \Gamma_{x_0 x} : V_0(u)(x) = v(u \circ \hat{\gamma}) < \infty\} .$$

In the sequel, we suppose that u has bounded path variation.

If u is a continuously differentiable function, then (1) allows to reformulate $V_0(u)$ as

$$V_0(u)(x) = \inf_{\gamma \in \Gamma_{x_0 x}} \int_0^L |D_\gamma u(\gamma(s))| ds . \quad (2)$$

Hence, $V_0(u)$ may be seen as a surface of minimal action for the potential $P = |D_\gamma u|$, the absolute value of the directional derivative of u in the tangent direction of the path.

The intuitive interpretation of the path variation is illustrated in Fig. 1: consider a particle moving along the graph of the function depicted on the left and starting at the source x_0 . Then, as shown on the right, the value of $V_0(u)$ evaluated at x represents the minimal sum of ascents and descents to be travelled to reach the point x .

The path variation expresses the same notion as the concept of *linear variation*, introduced in [19], though in a formulation without paths, as a part of a geometric theory for functions of two variables .

The *component* of u containing x , noted by K_x , designates the maximal connected subset of Ω such that $u(y) = u(x)$, $\forall y \in K_x$. The importance of the components for the path variation is given by the following proposition, whose proof is an immediate consequence of Def. 2.

Proposition 1. *The path variation acts on the components of the function:*

$$\forall x, y \in \Omega, K_x = K_y \Rightarrow \forall x_0, V_0(u)(x) = V_0(u)(y) .$$

Therefore, each element of an energy partition induced by the path variation is a union of components of the function. Thus, the operator that associates $\Pi(V(u), S)$ to a set of sources S is connected [32] and its application simplifies the image while preserving its geometrical structure.

In the discrete domain, the component structure of the function can be represented in a region adjacency graph. Hence, with this approach, the computation of the path variation is reduced to finding the path of minimal cost on a graph. This classical problem can be solved using a greedy algorithm [9, 20]. For a discrete definition of the path variation and implementation details, the reader is referred to [1].

3.2 Path Variation and Image Distance

In the context of mathematical morphology, the surface of minimal action associated to the potential $P = \|\nabla u\|$, given by the formula:

$$W_0(u)(x) = \inf_{\gamma \in \Gamma_{x_0 x}} \int_0^L \|\nabla u(\gamma(s))\| ds$$

was used to define the watershed transform in the continuous domain [26, 23]. If, as for the class of Morse functions, u has only isolated critical points, then W_0 induces a distance transform on Ω , called the *image distance* [26] or the *topographic distance* [23].

The relation between W and V in the regular framework is expressed by the following property:

Proposition 2. *If u is a Morse image, $u \in BPV(\Omega)$ and $x_0 \in \Omega$, then*

$$|u(x) - u(x_0)| \leq V_0(u)(x) \leq W_0(u)(x), \forall x \in \Omega .$$

In particular, if x and x_0 belong to a line of steepest slope for u , then

$$|u(x) - u(x_0)| = V_0(u)(x) = W_0(u)(x) ,$$

The proof of this proposition [1] follows from simple calculus and the fact that, by definition, $|D_{\dot{\gamma}}(u)| = \|\nabla u\|$ when $\dot{\gamma}$ is parallel to the gradient.

The behavior of these two energies can be compared using the test image shown on the right column of Fig. 2 and given by the simple formula $u(x) = c\|x - x_0\|$. The set of sources in this case is $S = \{x_0, x_1\}$, where x_0 is the upper left and x_1 the lower right corners of the domain. The central column

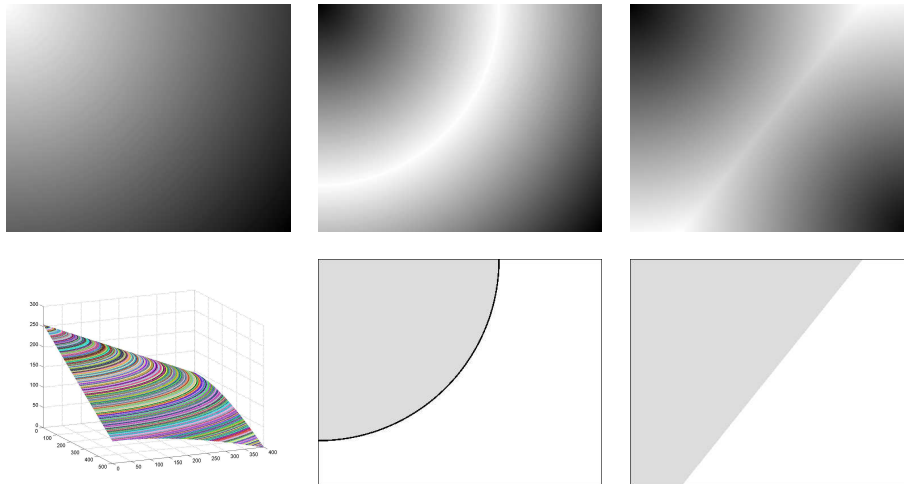


Fig. 2. From left to right. Top: u , $V_S(u)$ and $W_S(u)$. Bottom: Graph of u , energy partitions $\Pi(V(u), S)$ and $\Pi(W(u), S)$

shows the effect of the path variation: as a consequence of Prop. 1, u and $V_S(u)$ have in this example the same components and only their level is modified. The medial set $M(V(u), S)$, shown on black, is the component whose level is the average of the sources' levels. On the right column, we can observe that, since $\|\nabla u\|$ is constant, $W_S(u)$ is proportional to the Euclidean distance to the closest source and $M(W(u), S)$ corresponds to the medial line between the sources; however, in this example, the medial set falls in the intergrid space. Note that any other function for which $\|\nabla u\|$ is constant would produce the same partition $\Pi(W(u), S)$. This example illustrates how $\Pi(V(u), S)$, the partition induced by V , preserves the image structure better than $\Pi(W(u), S)$.

4 The Extrema Edges

4.1 The Extrema Partition

Surfaces of minimal action are often appropriated for a local level of analysis in the image. This is due to the fact that Def. 1 is based on an integration along the paths. Consequently, this type of energies may lose their meaning when the zones become too large. Besides, replacing a source $x_i \in S$ by another point $x'_i \in Z_i$ usually modifies the resulting energy partition.

Therefore, in order to construct an energy partition based on the path variation, the set of sources must be selected with care. Firstly, they should be physically representative of the image content. Secondly, each significant feature should contain at least one of them. Since they satisfy these conditions, the intensity extrema appear as natural candidates for the sources.

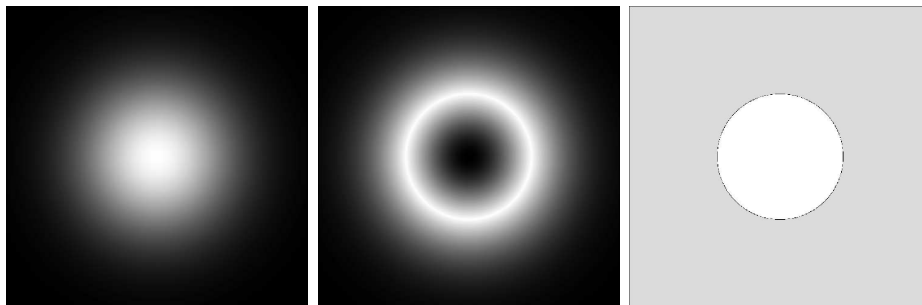


Fig. 3. Test image, energy end extrema partition.

Definition 4. The *extrema partition* of an image $u : \Omega \rightarrow \mathbf{R}$ is defined as $\Pi(V(u), \text{ext}(u))$, the energy partition induced by the path variation and the set of extremal components of u .

Thus, Prop. 1 implies that the elements of the extrema partition are unions of components of u . By definition, they can be divided in two types: on the one hand, the influence zones of the extrema, interpreted as the *atoms* or *elemental zones* of the image; on the other hand, the elements of the medial set $M(V(u), \text{ext}(u))$ are designated as *boundary components* of the atoms.

Figure 3 illustrates our approach on a simple regular case. The function u , on the left, is a Gaussian blob, where the only extremal components are the center and the border of the squared domain. The image on the middle shows the energy $V_{\text{ext}(u)}(u)$, rescaled by a factor of 2 for better visualization. On the right, the extrema partition $\Pi(V(u), \text{ext}(u))$ is composed by two elemental zones and a circular boundary component, fragmented by the quantization.

4.2 Definition of the Extrema Edges

The effects of the extrema partition on smooth functions, suggest the use of the boundary components to model the edges in the image. Nevertheless, in practice, digital images are subsampled on a discrete grid. Consequently, as noted in the previous examples, important parts of the medial set may fall in the intergrid space. An alternative to surround this problem is to consider an energy partition composed only by zones. Thus, the elements of the medial set that would fall exactly in the grid are assigned to one of their neighboring influence zones.

Then, an approximation of the image can be constructed by the assignation of a *model* to represent each influence zone. The model is determined by the distribution of the image values; simple models are the mean or median value in the zone, or the level at the source. When the model is constant, the valuation of each zone by its model produces a piecewise constant approximation of the image, referred in the sequel as a *mosaic image*. The mosaic corresponding to the extrema partition will be called the *extrema mosaic* of u . Generally, on real

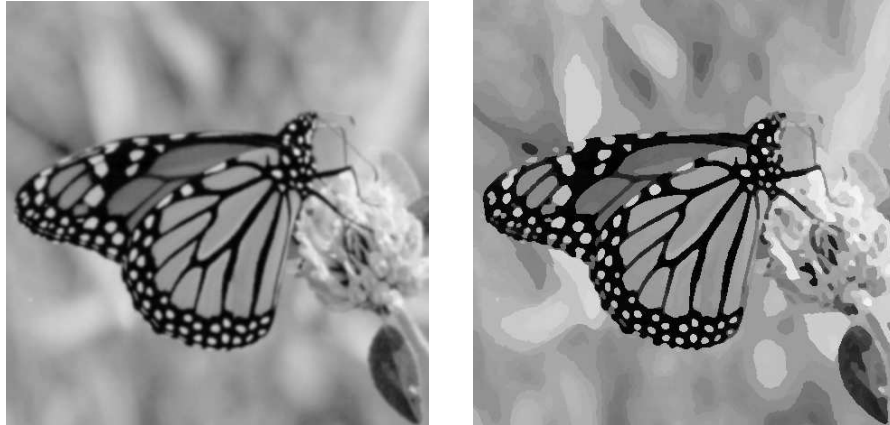


Fig. 4. Image and extrema mosaic.

images, the intensity at the extremum represents accurately the atom's levels. Hence, unless stated differently, this model was chosen.

The choice of the path variation as the energy and the spatial distribution of the intensity extrema provide a compromise between content conservation and simplification in the extrema mosaic. Perceptually, the effects of this piecewise constant approximation of the image can be better appreciated when the ratio between the number of components in the original image and the number of atoms is high. Figure 4 shows an example where this ratio is 68. On the left, we can observe the original image and, on the right, its extrema mosaic. This image illustrates well three important properties of our approach. First, a contrast enhancement in the butterfly's wings, mainly due to the choice of the zone model. Second, a reduction of the blur in the background, caused by the absorption of blurred contours and transition zones by neighboring atoms. Last, but not least, note how the boundaries of the atoms model accurately the contour information and, particularly, semantically important characteristics of edges such as corners and junctions. Therefore, they constitute a sound set of closed curves to search for edges in the image:

Definition 5. *The **extrema edges** of an image are defined as the discontinuities of its extrema mosaic.*

4.3 Extrema Edges and Watersheds

In mathematical morphology, the edges in an image u are usually modelled as the watershed lines of its gradient's modulus, $g = \|\nabla u\|$ [2, 31]. Their construction can then be obtained by a *flooding* process: a gradient image, seen as a topographical surface, is pierced at its regional minima and progressively immersed in water. The water floods uniformly the valleys, or catchment basins of

the minima, and, at the points where two lakes meet, a dam is built. When the surface is totally immersed, the union of the dams forms the watershed lines. This interpretation of the watershed transform inspired efficient algorithms for its implementation [34] and allowed the formalization of the watersheds in the continuous domain as the skeleton by influence zones of the image distance [26]. Furthermore, it suggested the interpretation of the minima of g as the dual concept of edges: the sources. In our notation, starting at a source $x_0 \in \Omega$, this energy can be written as

$$\widehat{W}_0(g) = W_0(g) + g(x_0) . \quad (3)$$

Thus, the energy associated to the segmentation by watersheds of an image u can be expressed as

$$\widehat{W}_{min(g)}(g) = \inf_{m_i \in min(g)} \widehat{W}_i(g) ,$$

where $min(g)$ denotes the set of regional minima of g . This continuous formulation motivated the implementation of the watersheds using the Fast Marching method [21].

Therefore, $\Pi(\widehat{W}(g), min(g))$, the energy partition associated to the watershed transform, has the following interpretation: the medial set $M(\widehat{W}(g), min(g))$ corresponds to the watershed lines of g and represent the edges in u . Besides, $Z(\widehat{W}(g), min(g))$, the zones of the minima, coincide with the lakes, or catchment basins of the topographical surface.

If we use V instead of W in (3), we obtain the following result, whose proof is based on Prop. 1 and 2 and the fact that, for Morse images, each catchment basin corresponds to the set of lines of steepest slope ending at its minimum [26].

Proposition 3. *If g is a Morse image and $g \in BPV(\Omega)$, then*

$$M(\widehat{V}(g), min(g)) = \bigcup_{x \in M(\widehat{W}(g), min(g))} K_x$$

Thus, the medial set of \widehat{V} coincides with the set of components of the watershed lines. Hence, in the continuous domain, the use of V on the gradient generally produces edges thicker than the watersheds.

In practice, as happens for the boundary components, the watersheds are usually fragmented in real images. Therefore, in order to compare the extrema edges and the watersheds, we used their corresponding mosaics. Indeed, the construction of both mosaics depends on the same factors: the digital connectivity, the gray level on the zones and the rule of assignation for the medial set. However, the fundamental difference is that the former is defined in the original image, while the latter is built on the modulus of its gradient. Consequently, the watershed lines depend also on the choice of a discrete approximation of the



Fig. 5. Above: original image and extrema mosaic. Below: mosaics of the energy partitions $\Pi(\widehat{W}(g), \min(g))$ and $\Pi(\widehat{V}(g), \min(g))$.

gradient. Moreover, a smoothing step is usually performed by most gradient operators in order to well pose differentiation [30, 10]. Since the smoothing implies a loss of information in the image content, the watersheds suffer from limited resolution in certain cases. These problems cannot be neglected in fields where the precision of the extracted features is an essential issue, as in medical image analysis.

Figure 5 depicts the mosaics associated to the different models of edges presented. The first row shows the original image, a detail of the *cameraman*, and the extrema mosaic. The second row depicts, on the left, the watershed mosaic constructed on the morphological gradient and, on the right, the mosaic corresponding to the choice of \widehat{V} as the energy and the gradient's minima as sources. For all the cases 8-connectivity was used, the zone model was the source's level

and the points in the medial set were assigned to the first source to reach them. As a consequence of the spatial distribution of the sources and their large number, all the methods preserve the main features in the scene, such as the silhouette of the man. However, the extrema mosaic enhances perceptually important details like the mouth or the inner parts of the camera that are lost in the mosaics of the second row. The loss of information is due to the absence of regional minima inside those features and, even if the result may be improved by changing the type of gradient operator or the connectivity, the problem is intrinsic to the use of the gradient image. Finally, since Prop. 3 implies that the partitions $\Pi(\widehat{W}(g), \min(g))$ and $\Pi(\widehat{V}(g), \min(g))$ differ mainly in their medial set, the two mosaics in the second row are almost identical.

5 Valuation of the Extrema Edges

Once a set of candidates for the edge points has been determined, the next problem is the integration of this local information into meaningful curves. In this section, we propose to construct a contrast driven hierarchy of partitions to provide global image information for the valuation of the extrema edges.

The idea of progressively merging regions of an initial partition has been used for a long time to address image segmentation problems [3, 15, 7, 13, 25]. In general, this type of methods can be implemented efficiently using a region adjacency graph (RAG), as described in [35, 11].

A RAG is an undirected graph where the nodes correspond to connected regions of the domain. The links encode the vicinity relation and are weighted by a *dissimilarity* measure. The dissimilarity δ is a function defined for every couple of neighboring regions. It takes values in an interval $I = [0, A]$, referred in the sequel as the set of *indices* or *scales*.

Then, removing the links of the RAG for increasing values of the dissimilarity and merging the corresponding regions produces a family of nested partitions, or hierarchy, $\{\mathcal{P}_\lambda\}_{\lambda \in I}$, where every region in \mathcal{P}_μ is a disjoint union of regions in \mathcal{P}_λ , for $\mu \geq \lambda$. Therefore, in this context, the selection of the initial partition and the dissimilarity measure determines the resulting hierarchy.

The watershed flooding provides a classical example of hierarchical segmentation: the gradient's modulus is again flooded from its minima but, instead of building a dam at the meeting points, the lakes merge. Increasing levels of water produce coarser partitions and the resulting hierarchy is known as the *dynamics* [12]. In terms of a region merging process, the initial partition is composed by the watershed mosaic and the dissimilarity is defined as the height of the saddle point between two adjacent lakes, i.e. the minimal value of the gradient in the common border of the regions [24].

Since our purpose was to construct a contrast driven hierarchy, the dissimilarity was measured on the initial partition and only boundary information was taken into account. Thus, we considered a local dissimilarity: the absolute value of the gray level difference of neighboring regions on the initial partition. Then, the dissimilarity was defined as a function of the local dissimilarities' distribu-



Fig. 6. Extrema mosaic and segmentation for the scale $\lambda = 54$.

tion in the common boundary of the regions. For the examples presented in this paper, the dissimilarity was the average of the local dissimilarities. The resulting hierarchy is noted by \mathcal{H} .

Figure 6 illustrates the application of \mathcal{H} . The left image displays the initial partition, the extrema mosaic of the *cameraman*. On the right, we can observe the segmentation corresponding to the scale $\lambda = 54$. Note how \mathcal{H} expresses the perceived contrast in the image; at the scale presented, only contrasted regions remain in the segmentation, regardless of their size.

In order to measure the relevance of the extrema edges, the notion of *saliency image* of a hierarchy presents a particular interest:

The *saliency* of a pixel, with respect to a hierarchy of partitions $\{\mathcal{P}_\lambda\}_{\lambda \in I}$, is defined as the highest index λ for which the pixel belongs to a boundary of \mathcal{P}_λ . The valuation of each pixel by its saliency determines a *saliency image*. The saliency image provides a compact description of the hierarchy: a threshold λ in this image supplies the set of boundaries of the corresponding partition \mathcal{P}_λ . Thus, the usefulness of the saliency image is determined by the hierarchy. The saliency image of the dynamics hierarchy was used in [28] to valuate the watersheds.

Definition 6. The *valuated extrema edges* of an image u correspond to the saliency image associated to the hierarchy \mathcal{H} , when the initial partition is the extrema mosaic of u .

The left image of Fig. 7 shows the valuated extrema edges of the *cameraman*, while the right image displays the threshold corresponding to the scale $\lambda = 54$.

The main properties of our edge model may be summarized as follows. First, the valuation is obtained using global contrast information and a simple threshold in the valuated extrema edges determines a set of meaningful closed curves.

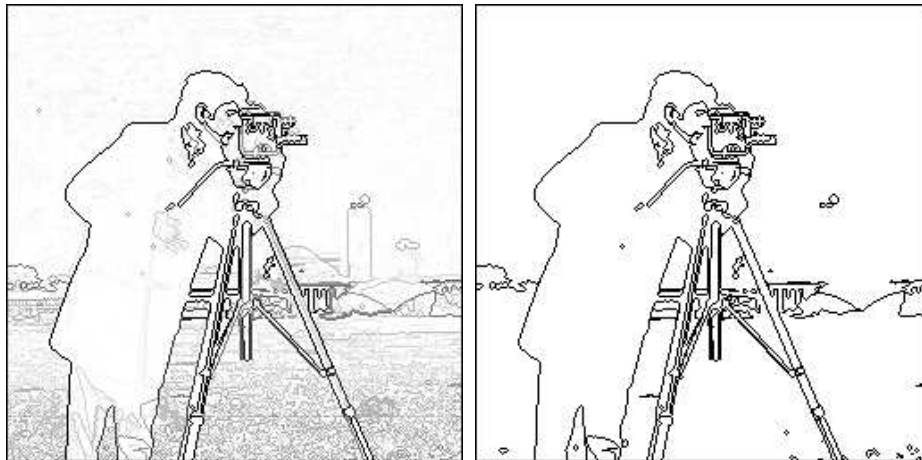


Fig. 7. Valuated extrema edges and threshold for $\lambda = 54$.

Second, the location of edges is conserved through the scales. Last, but not least, the use of the extrema mosaic preserves the geometric structure of the original image and enhances the semantically important characteristics of edges.

Note that \mathcal{H} can also be applied directly to the original image; however, the use of the extrema mosaic generally improves the quality of the edges obtained. Figure 8 shows an application to medical image analysis where the use of the extrema mosaic as the initial partition is a crucial issue. The goal was to detect a pathology called the *drusen* - the dark spots - in images of the eye fundus, as the one shown on the top left. The variations in the background's intensity in retinal angiographies as well as the absence of abrupt discontinuities in the drusen boundaries make their extraction a difficult problem with classical edge detection methods. The top right image shows the *saliency image* associated to \mathcal{H} when the initial partition is the original image. The image was rescaled for better visualization, but the scale Λ at which a single region remains is only 6. Since the transitions in the original image are smooth, the saliency image produces blurred edges. In contrast, the second row depicts the application of the extrema edges. On the left, we can observe the extrema mosaic, where the drusen can be clearly distinguished from the background. The right image depicts the valuated extrema edges, where $\Lambda = 58$. Note how the method provides the location and the shape of the drusen with precision. Furthermore, their saliency may be used to evaluate the magnitude of the disease.

6 Conclusion and Perspectives

We presented a new approach to model edges in the image. The method is divided in two parts. First, a set of possible edge points, the extrema edges, is defined and then a measure of saliency is assigned to every point in this set. The

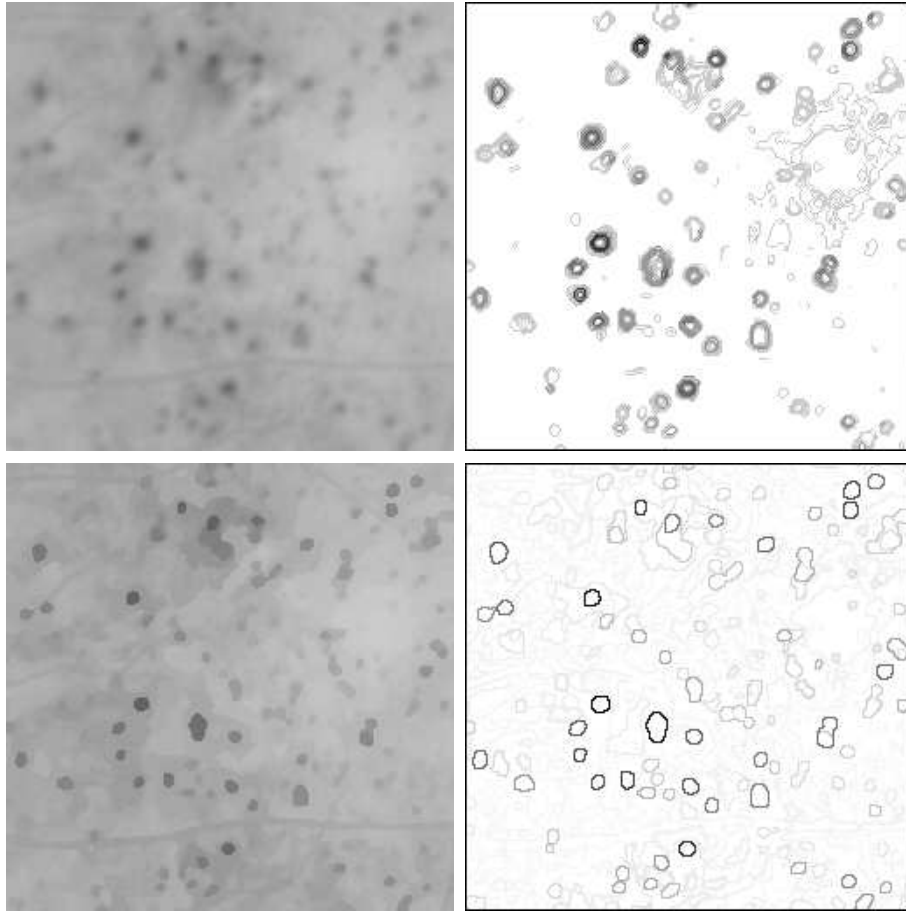


Fig. 8. Row 1: original image and saliency image. Row 2: extrema mosaic and valuated extrema edges.

extrema edges are defined as the discontinuities of the mosaic image associated to the energy partition $\Pi(V(u), ext(u))$. Their valuation is obtained using global information through a family of nested partitions guided by a notion of contrast. The method uses only the original image to construct a contour map called the *valuated extrema edges*. A threshold in this image provides a set of closed curves where semantically important characteristics of edges are preserved.

Finally, this paper focused on monochrome images in order to emphasize the mathematical formulation of our approach and to establish a comparison with the continuous watershed transform. Nevertheless, a straightforward application to color images can be done by considering only their lightness channel. Alternatively, we are presently working on the generalization of our approach to vector-valued images.

References

1. P. A. Arbeláez. The path variation. Technical report, CEREMADE, 2003.
2. S. Beucher and F. Meyer. The morphological approach to segmentation: The watershed transformation. *Mathematical Morphology in Image Processing*, pages 433–481, 1992.
3. C. R. Brice and C. L. Fenema. Scene analysis using regions. *Artificial Intelligence*, 1:205–226, 1970.
4. J. Canny. A computational approach to edge detection. *IEEE Transactions on Pattern Analysis and Machine Intelligence*, 8(6):679–698, November 1986.
5. L. D. Cohen. Multiple contour finding and perceptual grouping using minimal paths. *Journal of Mathematical Imaging and Vision*, 14(3):225–236, 2001.
6. L. D. Cohen and R. Kimmel. Global minimum for active contour models: A minimal path approach. *International Journal of Computer Vision*, 24(1):57–78, August 1997.
7. L. D. Cohen, L. Vinet, P. Sander, and A. Galalowicz. Hierarchical region based stereo matching. In *Proc. 6th Scandinavian Conference on Image Analysis*, 1989.
8. T. Deschamps and L. D. Cohen. Fast extraction of minimal paths in 3d images and applications to virtual endoscopy. *Medical Image Analysis*, 5(4):281–299, 2001.
9. E. W. Dijkstra. A note on two problems in connection with graphs. *Numerische Mathematik*, 1:269–271, 1959.
10. D. A. Forsyth and J. Ponce. *Computer Vision: A Modern Approach*. Prentice Hall, 2003.
11. L. Garrido, P. Salembier, and D. Garcia. Extensive operators in partition lattices for image sequence analysis. *Signal Processing*, 66(2):157–180, April 1998. Special Issue on Video Sequence Segmentation.
12. M. Grimaud. New measure of contrast: Dynamics. In *Image Algebra and Morphological Processing III*, SPIE, San Diego, CA., 1992.
13. R. Haralick and L. Shapiro. *Computer and Robot Vision*, volume I. Adison Wesley, 1992.
14. E. Hewitt and K. Stromberg. *Real and Abstract Analysis*. Springer Verlag, 1969.
15. S. L. Horowitz and T. Pavlidis. Picture segmentation by a directed split-and-merge procedure. In *Proceedings of the Second International Joint Conference on Pattern Recognition*, pages 424–433, 1974.
16. C. Jordan. Sur la série de fourier. *C. R. Acad. Sci. Paris Sér. I Math.*, 92(5):228–230, 1881.
17. R. Kimmel and A. M. Bruckstein. Global shape from shading. *CVIU*, 62(3):360–369, 1995.
18. R. Kimmel, N. Kiryati, and A. M. Bruckstein. Distance maps and weighted distance transforms. *Journal of Mathematical Imaging and Vision*, 6:223–233, May 1996. Special Issue on Topology and Geometry in Computer Vision.
19. A. S. Kronrod. On functions of two variables. *Uspehi Mathematical Sciences*, 5(35), 1950. In Russian.
20. R. Kruse and A. Ryba. *Data structures and program design in C++*. Prentice Hall, New York, 1999.
21. P. Maragos and M. A. Butt. Curve evolution, differential morphology and distance transforms applied to multiscale and eikonal problems. *Fundamenta Informaticae*, 41:91–129, 2000.
22. D. Marr and E. Hildreth. Theory of edge detection. In *Proc. of Royal Society of London*, volume B-207, pages 187–217, 1980.

23. F. Meyer. Topographic distances and watershed lines. *Signal Processing*, 38:113–125, 1994.
24. F. Meyer. Hierarchies of partitions and morphological segmentation. In Michael Kerckhove, editor, *Scale Space and Morphology in Computer Vision*, pages 161–182, 2001.
25. J. M. Morel and S. Solimini. *Variational Methods in Image Segmentation*. Birkhauser, 1995.
26. L. Najman. *Morphologie Mathématique: de la Segmentation d'Images à l'Analyse Multivoque*. PhD thesis, Université Paris Dauphine, 1994.
27. L. Najman and M. Schmitt. Watershed of a continuous function. *Signal Processing*, 38(1):99–112, July 1994.
28. L. Najman and M. Schmitt. Geodesic saliency of watershed contours and hierarchical segmentation. *IEEE Transactions on Pattern Analysis and Machine Intelligence*, 18(12):1163–1173, 1996.
29. I. P. Natansson. *Theory of Functions of a Real Variable*. Frederick Ungar Publishing, New York, 1964.
30. J. R. Parker. *Algorithms for Image Processing and Computer Vision*. John Wiley and Sons, 1997.
31. M. Schmitt and J. Mattioli. *Morphologie Mathématique*. Masson, 1994.
32. J. Serra and P. Salembier. Connected operators and pyramids. In SPIE, editor, *Image Algebra and Mathematical Morphology*, volume 2030, pages 65–76, San Diego CA., July 1993.
33. J. A. Sethian. *Level Set Methods and Fast Marching Methods*. Cambridge University Press, Cambridge, UK, 2 edition, 1999.
34. L. Vincent and P. Soille. Watersheds in digital spaces: an efficient algorithm based on immersion simulations. *PAMI*, 13(6):583–598, 1990.
35. T. Vlachos and A. G. Constantinides. Graph-theoretical approach to colour picture segmentation and contour classification. In *IEE Proc. Vision, Image and Sig. Proc.*, volume 140, pages 36–45, February 1993.